

# Lighting correction for underwater mosaicking enhancement

Manon BORGETTO, Vincent RIGAUD and Jean-François LOTS

IFREMER\*, DNIS/SM/RNV department, Toulon, France

## Abstract

Realtime mosaic creation is one of the most developing areas in recent underwater research. Mosaics are built from an image sequence acquired with an underwater vehicle which carries a camera. Usually, such vehicles dive deeply (up to 6,000 meter depth). Due to the lighting conditions, halo effects and illumination widespread, the light supplied is non-uniformly distributed. Solving that problem during a preprocessing step should improve both image quality and mosaic creation. This paper presents two methods which improve the lighting problem. The first one is the homomorphic filtering and the second one relies on the determination of a reference image by original methods. Several experiments on real underwater images have been carried out to demonstrate the validity of the proposed approaches.

**Keywords:** underwater mosaics, intensity enhancement, lighting correction, homomorphic filtering, radiometric correction.

## 1 Introduction

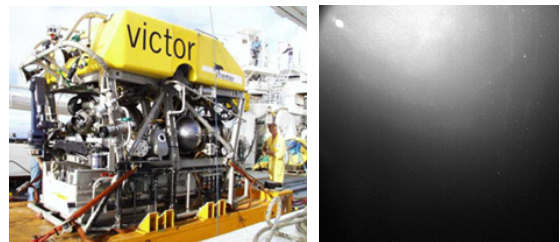
Realtime mosaic creation is one of the most developing areas in recent underwater research. One of this research's goals is to obtain image mosaics, which can for instance provide a visual map of wrecks, pipes and more generally underwater structures and natural areas [5, 12].

In our case, mosaics are built from an image sequence by an estimation of the motion parameters [8]. This image sequence is acquired by a Remotely Operated Vehicle (ROV) (see figure 1(a)). A camera is attached to the vehicle and self-calibrated [9]. As the ROV dives deeply (6,000 meter deep), artificial lighting conditions constrain our results. The vehicle is typically flying five meters above the seabed so that artificial light produces non-uniform lighting on the images: the center of the image is very bright while the surrounding area is darker (see figure 1(b)). This non-uniformity of lighting

has an obvious impact on the mosaic creation process. Correcting these adverse lighting effects should improve the quality of the mosaics.

Two methods of correction were investigated: radiometric correction and reflectance-illumination modelling of a digital image.

This article is organized as follows. Firstly, a brief summary on image mosaicking is presented. Then histogram equalization, a classical regularization method is recalled, then the radiometric correction is explained, and finally homomorphic filtering is presented. Secondly, experimental results obtained with the application of the aforementioned methods on real data are discussed. We then conclude our investigations.



(a) The ROV Victor 6000

(b) Non-uniform lighting

Figure 1: The ROV Victor 6000 (a) and an example of non-uniform artificial lighting (b)

## 2 Image mosaicking

An image mosaic is a panoramic view of a site of interest, allowing the site to be observed and studied as a whole. Underwater, obtaining mosaics is of a greater importance to scientists since the field of view is limited by the non-uniform lighting provided by the spotlights. The creation of the mosaic relies on two steps: registration between

\* IFREMER = Institut Français de Recherche pour l'Exploitation de la MER

successive images (computation of an interimage transformation) and rendering. The quality of a mosaic relies on the accuracy of the juxtaposition between the images of the video sequence.

A few methods will be presented in the following. The methods from Marks *et al.* [6] and Santos-Victor *et al.* [13] are quite similar, except that the first one works in real-time whereas the second one does not, but is more robust and more precise. These two methods are based on the following four steps:

- Image filtering and feature extraction.
- Feature matching.
- Motion estimation (transformation between successive images estimation).
- Rendering.

The first step is realized in the first method with a Laplacian of Gaussian filter (edge detector), whereas the second method uses a Harris extractor (corner detector). The second step relies on a correlation between each image feature and a window situated in the following image, at the same position. The motion estimation is processed by estimating a 4 parameter motion model ([6]) or a 8 parameter motion model ([13]). The rendering step consists in fusing the new image with the mosaic already processed, thanks to the registration parameters (translation, rotation and scale).

The "Robust MultiResolution" (RMR)<sup>1</sup> method proposed by Odobez and Bouthemy [7] relies on the same 4 steps. Their idea is to use a gaussian pyramid for each image (bottom level: original image, top level: less resolution image). They first estimate the motion at the top level and refine it by descending the levels. The motion estimation is done thanks to a robust estimator (M-estimator). Then the rendering is processed.

In the next section, we present the different methods of lighting correction we investigated.

## 3 Lighting effect correction in underwater environment

### 3.1 Histogram equalization

Histogram equalization is a well-known technique in the area of image enhancement [10, 2]. This technique modifies the gray value repartition of an image. The idea is to equally represent each gray value intensity by making the

<sup>1</sup>This method is integrated in the IFREMER's mosaic creation MATISSE®software.

resulting image histogram flat. The image is associated to a probabilistic modelling whose histogram represents the probability density of the gray level variable. The image of gray level intensity  $I_0(i, j)$  is considered as a set of realizations of a random variable  $X$  (corresponding to a gray level variable).

Let

- $f_X(x)$  be the probability density of  $X$
- $F_X(x) = \int_{x_{min}}^x f(x)dx$  be the repartition function of  $X$

$f_X$  represents the normalized histogram while  $F_X$  represents the cumulative histogram. One researches a transformation  $\phi$  uniform and strictly increasing such as random variable  $Y$  (corresponding to the transformed gray level variable) follows:

$$Y = \phi(X) \sim \mathcal{U}_{[y_{min}, y_{max}]}$$

with

- $f_Y(y) = \frac{1}{y_{max} - y_{min}} \mathbb{1}_{[y_{min}, y_{max}]}$
- $F_Y(y) = \frac{1}{y_{max} - y_{min}} y \mathbb{1}_{[y_{min}, y_{max}]}$

where

$$\mathbb{1}_{[y_{min}, y_{max}]} = \begin{cases} 1 & \forall y \in [y_{min}, y_{max}] \\ 0 & \text{otherwise} \end{cases} \quad (1)$$

The transformation  $\phi$  is then defined by the following expression for  $x \in [x_{min}, x_{max}]$  [2]:

$$\phi(X) = (y_{max} - y_{min})F_X(x) + y_{min} \quad (2)$$

Let  $n$  be the number of pixels in the image and  $n_x$  be the number of pixels whose gray level is  $x$ .

We estimate the histograms  $f_X(x)$  and  $F_X(x)$  by the following expressions:

- $f_X(x) = \frac{n_x}{n}$
- $F_X(x) = \frac{\sum_{k=x_{min}}^x n_k}{n}$

Let  $I_e$  be the variable representing the equalized intensity value and  $n_{gray}$  be the number of gray levels (usually 256).

By replacing the expressions in equation 2, the transformation which guarantees that the pixels of the resulting image  $I_e(i, j)$  follows an uniform law is the following:

$$i_e(i, j) = (n_{gray} - 1) \cdot F_X [i_o(i, j)] \quad (3)$$

One then only has to transform each pixel intensity by applying equation 3.

### 3.2 CCD camera radiometric correction

This method relies on the CCD camera radiometric correction, mostly used in remote sensing and astronomical imaging [14]. The model can be written as follows:

$$I_a(x, y) = g(x, y) \cdot I_{wp}(x, y) + I_d(x, y) + I_t(x, y) \quad (4)$$

where

- $I_a(x, y)$  is the acquired image
- $I_{wp}(x, y)$  would be the pixel intensity if the image was taken without any perturbation
- $I_d(x, y)$  is the darkness reference image (**DR** image), taken with a closed camera objective
- $g(x, y)$  is the reference image corresponding to an uniformly lit image (**ULR** image for Uniformly Lit Reference image)
- $I_t(x, y)$  corresponds to the temporal transmission noise between the camera and the acquisition card. It corresponds to a gaussian centered noise. It has small values but can not be estimated. For sake of simplicity, it will be neglected from now on.

Equation 4 can be written as:

$$I_{wp}(x, y) = \frac{I_a(x, y) - I_d(x, y)}{g(x, y)} \quad (5)$$

To implement that method, we have to estimate the **DR** image and the **ULR** image.

The **DR** image is acquired by closing the camera objective. On the one hand, the camera sensitivity is supposed uniform. On the other hand, this **DR** image depends on the environmental conditions such as pressure and temperature. In practice, the camera is relatively cold in deep sea (less than 10 °C) so the **DR** image has small values. Furthermore, it is not simple to acquire that image in deep water because the camera is not occultable. For all these reasons, the contribution of the **DR** image is omitted.

The underwater images used for our experiments are mostly collected on sandy seabeds. The **ULR** image would correspond to a seabed image acquired with two HMI<sup>2</sup> spotlights (at least) on the sand alone (no object on the seabed). Unfortunately there are always objects such as algae or rocks on the seabed. So we cannot acquire this image in that manner. Despite these issues, we can estimate this image through the following methods.

---

<sup>2</sup>HMI is a halide spotlight whose radiometric properties underwater are similar to those of daylight.

#### 3.2.1 Convolution with a gaussian filter

The first basic idea is to obtain this **ULR** image by convolving each image of the sequence with a gaussian filter. This yields a smoothed image, which should correspond to the expected **ULR** image and could be used for the division in equation 5. The **ULR** image is updated for each image in the sequence.

#### 3.2.2 Finding a "natural" reference image

The second way to find out the reference image is to acquire an image while diving. This image has to be acquired in deep water in order to possess the same lighting conditions as on the seabed because of the darkness and the spotlight illumination performances.

The third direction we investigated was to acquire an image of the seabed by tuning the focal up to infinity (*i.e.* defocalised). By acquiring the **ULR** image that way, we ensure that the image will be smoothed so that the object edges will not be visible and that the predominant lighting will remain. It is almost equivalent to convolve the image with a gaussian filter.

#### 3.2.3 Lighting modelling

Another way to find out the reference image is to search a model of the lighting. As the lighting seems to be isotropic and quite elliptic, we propose to model it by a gaussian based on an elliptic area. For this method, the operator plots a limit of the lighting in the image (for example, the white curve plotted in figure 6(c)) in order to estimate the elliptic parameters through an interpolation of the plotted curve points [3]. Once that is done, the operator has to adjust the gaussian parameters to obtain the qualitatively best reference image.

We presented three methods to determine a reference image which modelled the lighting. In the following section, we will present another approach relying on a study of the frequencies repartition in the image.

### 3.3 The illumination-reflectance modelling of an image

This method [1, 4, 10] assumes that an image can be separated into two components: reflectance and illumination. Actually, illumination varies continuously and slowly through the image while reflectance can vary abruptly on object edges. The low frequencies in the image cover illumination effects while the high frequencies cover reflectance effects. The idea is thus to bring both compo-

nents apart.

Let

- $f(x, y)$  be the image intensity function,
- $i(x, y)$  be the illumination component,
- $r(x, y)$  be the reflectance component.

If we neglect the temporal transmission noise and the darkness image, equation 4 can be simply rewritten as follows:

$$f(x, y) = i(x, y)r(x, y) \quad (6)$$

We have to dissociate both terms in order to handle them separately with a frequency filter. For that, we can first write equation 6 as follows:

$$\ln f(x, y) = \ln i(x, y) + \ln r(x, y) \quad (7)$$

Secondly, we apply the Fourier Transform (**FT**) to equation 7 to obtain:

$$F(u, v) = I(u, v) + R(u, v) \quad (8)$$

where

- $F(u, v) = \mathbf{FT}\{\ln f(x, y)\}$
- $I(u, v) = \mathbf{FT}\{\ln i(x, y)\}$
- $R(u, v) = \mathbf{FT}\{\ln r(x, y)\}$

In order to separate both terms, one designs a frequency filter  $H(u, v)$  which reduces the illumination component contribution and raises the reflectance component contribution (object edges).

Let  $F'$  be the **FT** of the so-filtered image.

$$\begin{aligned} F'(u, v) &= F(u, v)H(u, v) \\ &= I(u, v)H(u, v) + R(u, v)H(u, v) \end{aligned} \quad (9)$$

Once that filter is designed and processed with the image  $F'$ , the corrected image is obtained by applying the inverse Fourier Transform and taking the exponential of the result. [1] proposed a high pass homomorphic filter for the choice of  $H$ . The chosen frequency filter is a FIR (Finite Impulse Response) high pass filter proposed by a software package (Matlab©). The algorithm relies on the Parks-McClellan algorithm [11]. An example of the filter is shown on figure 2.

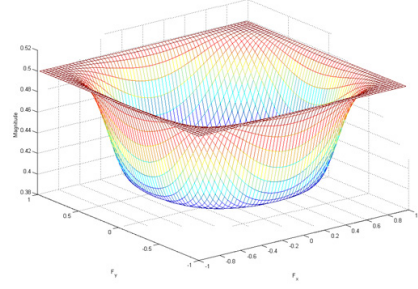


Figure 2: An example of the Parks-McClellan filter

## 4 Experimental results

The different methods were tested on real underwater images. A sequence of amphorae was acquired 300 meter deep in the Mediterranean Sea. A plane wreck was photographed 1,200 meter deep in the Mediterranean Sea again. No image sequence of this airplane was taken. A preprocessing could be applied to these images but no mosaics could be created because of the poor overlap between the images of the plane.

The images present a bright halo while the surrounding area is darker and objects in this area are less visible. In this paper, results are evaluated qualitatively. Indeed, no quality index is available today for these image processing techniques. However, some visual parameters are taken into account, such as the halo attenuation and the dark area brightening.

We assumed that the mosaic creation should be enhanced by first enhancing each image's quality. Notice that intensity manipulations will have an impact on the mosaics processed by the RMR [8].

### 4.1 Histogram equalization

For this method, we used the amphorae sequence. This method is known to be image-dependent. The histograms in figures 3(c) and 3(d) show that the gray levels of image 3(b) are better distributed. However the spatial result in figure 3(b) is not satisfying. Indeed, the bright halo is emphasized whereas the opposite effect was sought. The histogram is not a good mean to evaluate the underwater image quality enhancement and is not the quality index we would like to have in order to evaluate the image quality.

As mentioned previously, the motion estimated by the RMR method is influenced by the intensity ma-

nipulation such as histogram equalization. Indeed the resulting mosaic 3(f) is larger than the initial mosaic 3(e).

In spite of the better histogram quality, image and mosaic quality has not been enhanced (see figure 3(a) and 3(b)). Therefore this method is not adapted to underwater images.

## 4.2 Radiometric correction

### 4.2.1 Building a "convolved" reference image

Each convolved image is obtained by convolving a raw image with a gaussian filter (section 3.2.1) whose parameters are chosen by an operator. We notice that applying the radiometric correction with the convolved image corresponding to the raw image to be treated improves each image's quality. Indeed, in figure 4(c), the lighting is more uniform and the halo has disappeared. However, the mosaic built from these images is not visually enhanced (see figure 4(e)). The RMR method is very sensitive to the lighting changes. As this method does not work as well as expected, we try to use in the following a natural reference image to obtain the lighting.

### 4.2.2 Finding a "natural" reference image

We used an image taken during a ROV Victor 6000's dive. Images of a plane wreck were acquired during a 1,200 meter deep dive (see figures 5(a) and 6(a)). A bright halo and a darker area are well noticeable. The image acquired during the dive (section 3.2.2) is image 5(b). As we can see in picture 5(c), the images are enhanced and more details of the airplane than in the original images are distinguishable.

The third method of acquiring the **ULR** image, mentioned in 3.2.2: tuning up the focal to infinity, is a preliminary idea that should be operated next year during a operational cruises.

### 4.2.3 Lighting modelling

For this method, we choose to use the airplane images because the halo was easy to work out and the ellipse to plot. We modelled the lighting by a gaussian based on an elliptic plane. The operator first delimited the bright halo by a white curve. That gave a list of points. From this list, the elliptic parameters were estimated by an optimization process. Then the gaussian parameters were adjusted by the operator in order to obtain the most enhanced image result. On figure 6(d), we can see that the parameterization could be enhanced. However, this

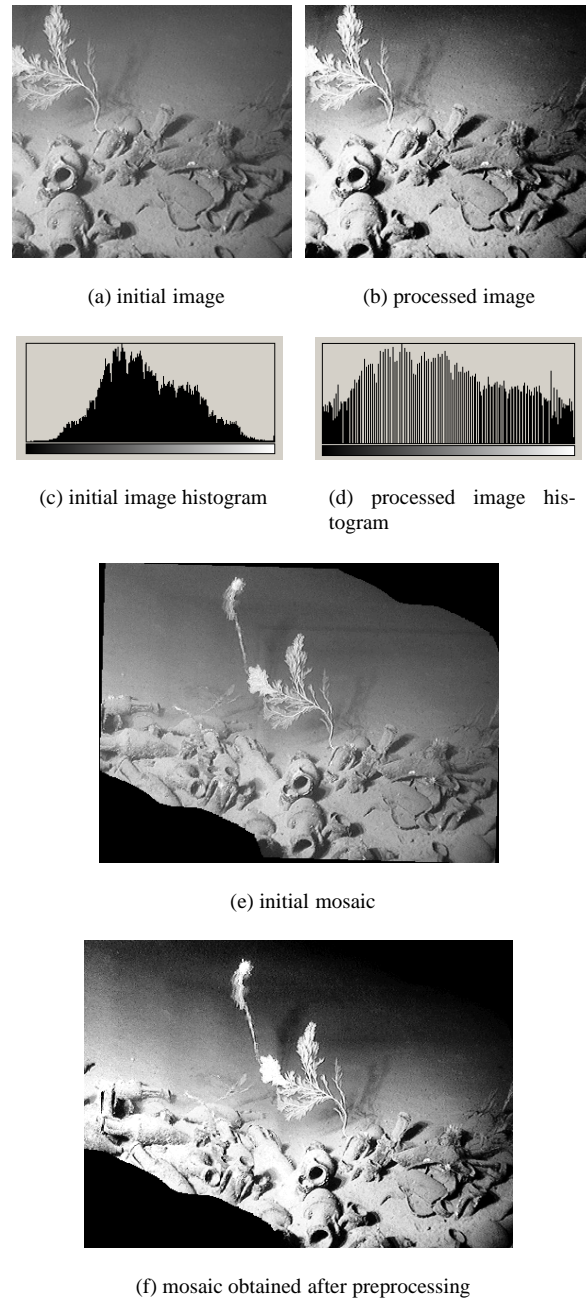
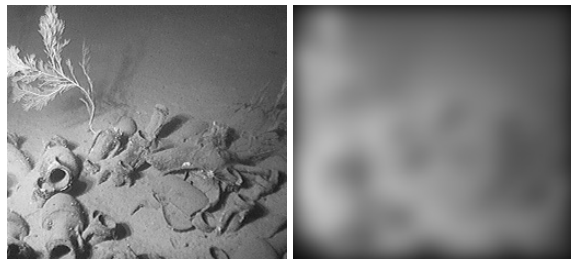


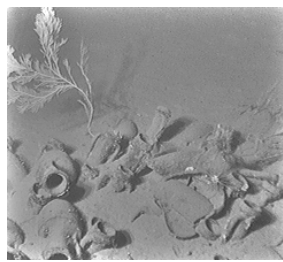
Figure 3: Basic histogram equalization with poor results

method is still promising.

At the moment, a human intervention is required to delimit the bright halo. The automation of the plotting of the delimited area and the estimation of the gaussian parameters will constitute further work.



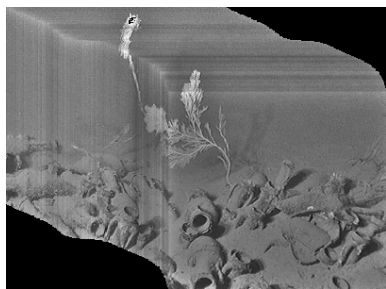
(a) initial image (b) reference convolved image



(c) processed image

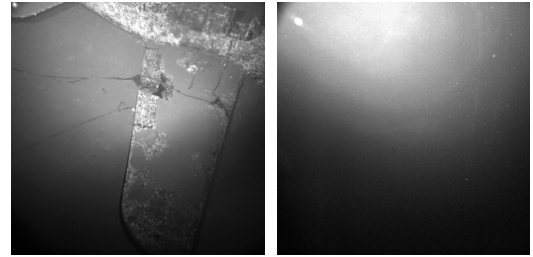


(d) initial mosaic

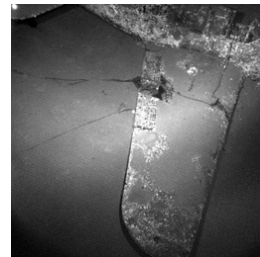


(e) mosaic built with processed images

Figure 4: Radiometric correction: convolution with a gaussian filter

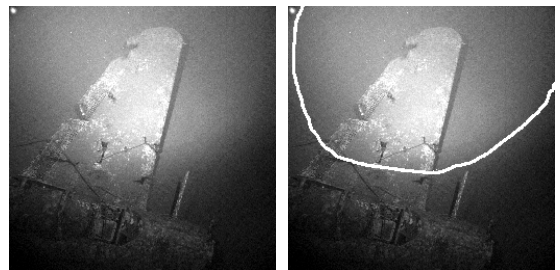


(a) initial image (b) image acquired during the dive

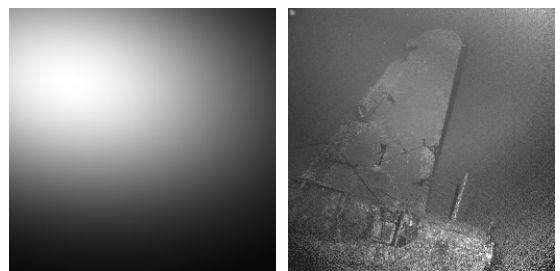


(c) processed image

Figure 5: Radiometric correction: correction with the image taken while diving



(a) initial airplane image (b) airplane halo tracing



(c) elliptic modelling (d) processed image

Figure 6: Radiometric correction: correction with the elliptic gaussian modelling

### 4.3 Radiometric correction in brief

Using natural halo images (dive image or tuning up the focal to infinity image) is a promising method. Indeed, only one particular image has to be acquired before taking the image sequence and no further processing is required. Acquiring this image should not be a problem for the ROV Victor 6000.

The lighting modelling requires a human operator but automation is going to be implemented. The advantage is that no image has to be acquired before taking the image sequence, but the drawback is that, as any models, it is an approximation of reality.

### 4.4 Homomorphic filtering

We calculated the homomorphic filter parameters qualitatively, that is we looked each time at the resulting image quality. As noticed at the beginning of this section, we have no mean to work out the parameters automatically on quantitative considerations. As we can see on the processed image of the airplane, 7(b), and the processed image of the amphorae, 7(d), the result of the preprocessing step seems to have better quality than the original image: the bright halo is less visible, the illumination seems to be more homogeneous and the airplane details which were in the dark are now visible. Furthermore, the amphorae mosaic 7(f) has a good visual quality. The method gives satisfying results in that respect.

## 5 Conclusions

In this paper, we investigated several methods on real underwater images.

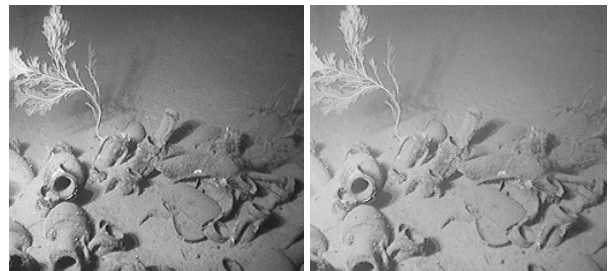
First, several methods were investigated to obtain a reference image.

- The first one is the result of a convolution between a gaussian filter and the image. This image is not the same for all images but is built for each image. It yields satisfying results for each image, but the mosaic is not enhanced.
- The second reference image is acquired in a "natural" way. Indeed, this image can be acquired during the dive or by tuning up the focal to infinity. Acquiring this image during the dive gives promising results. Tuning up the focal to infinity has not been operated yet, but will be operated during future cruises. No mosaic could be created because no image sequence was taken. Only photos were available.



(a) initial image

(b) processed image

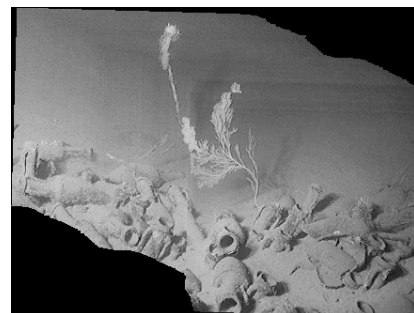


(c) initial image

(d) processed image



(e) initial mosaic



(f) mosaic built with processed images

Figure 7: Homomorphic filtering

- The third way to build this reference image is to model the bright halo by a gaussian based on an elliptic plane. This method is promising but needs to be automated. This will be done in a future work.

Second, the homomorphic filtering yields good results regarding each image and the mosaics but has to be automated because the filter parameters are chosen by the operator.

Real time implementation of the most promising methods will be experimented on our MATISSE<sup>®</sup><sup>3</sup> (see website [15]) online mosaic construction software during operational cruises in 2003.

#### Acknowledgements:

This MSc work was funded by IFREMER.

We are grateful to IFREMER for providing us the use of MATISSE<sup>®</sup> to create mosaics with the RMR algorithm engineered by INRIA [8].

## References

- [1] H.G. Adelman. Butterworth equations for homomorphic filtering of images. *Computers in Biology and Medicine*, 28:169–181, 1998.
- [2] J.-P. Cocquerez and S. Philipp. *Analyse d'images : filtrage et segmentation*. Enseignement de la physique. Masson, 1995.
- [3] A. Fitzgibbon, M. Pilu, and R.B. Fisher. Direct least square fitting of ellipses. *IEEE Transactions on Pattern Analysis and Machine Intelligence*, 21(5):476–480, May 1999.
- [4] R.C. Gonzales and R.E. Woods. *Digital image processing*. Addison Wesley, 1992.
- [5] N. Gracias and J. Santos-Victor. Underwater video mosaics as visual navigation maps. *Computer Vision and Image Understanding*, 79(1):66–91, July 2000.
- [6] R. Marks, S. Rock, and M. Lee. Real-time video mosaicking of the ocean floor. *IEEE Journal of Oceanic Engineering*, 20(3):229–241, July 1995.
- [7] J.-M. Odobez and P. Bouthémy. Estimation robuste multiéchelle de modèles paramètres de mouvement sur des scènes complexes. *Traitement du signal*, 12(2):113–128, 1995.
- [8] J.-M. Odobez and P. Bouthémy. Robust multiresolution estimation of parametric motion models. *Journal of Visual Communication and Image Representation*, 6(4):348–365, December 1995.
- [9] Nathalie Pessel. Auto-calibrage d'une caméra en milieu sous-marin. 16èmes Journées Jeunes Chercheurs en Robotique, Lyon, September 2002.
- [10] William K. Pratt. *Digital image processing*. Wiley, 1991.
- [11] L.R. Rabiner, J.H. McClellan, and T.W. Parks. FIR digital filter design techniques using weighted Chebyshev approximations. *Proceedings of IEEE*, 63(4):595–610, April 1975.
- [12] Vincent Rigaud. Underwater mosaicking. IARP, International Workshop on Underwater Robotics for Sea Exploitation and Environmental Monitoring, October 2001. Rio de Janeiro, Brasil.
- [13] J. Santos-Victor, N. Gracias, and S. van der Zwaan. Using vision for underwater robotics: video mosaics and station keeping. IARP, International Workshop on Underwater Robotics for Sea Exploitation and Environmental Monitoring, October 2001. Rio de Janeiro, Brasil.
- [14] J.P. Tarel. Calibration radiométrique de caméra. Technical report, INRIA, Mars 1995.
- [15] IFREMER website. Matisse, 2001. url : <http://www.ifremer.fr/flotte/r&d/mosaique.htm>.

---

<sup>3</sup>MATISSE = Mosaïque Assistée par Traitement d'ImageS et de Sources Externes - external source and image processing assisted mosaics